SCIENTIFIC REPORTS

OPEN

SUBJECT AREAS:
TUMOUR SUPPRESSORS
CNS CANCER
BIOMARKER RESEARCH
DNA DAMAGE RESPONSE

Received
13 September 2012

Accepted
10 December 2012

Published
29 January 2013

Correspondence and requests for materials should be addressed to A.N. (akiranak@chiba-cc.jp)

* These authors contributed equally to this work.

Temozolomide suppresses *MYC* via activation of TAp63 to inhibit progression of human glioblastoma

Tomohiro Yamaki[1,2]*, Yusuke Suenaga[1]*, Toshihiko Iuchi[3], Jennifer Alagu[1], Atsushi Takatori[1], Makiko Itami[4], Akinobu Araki[4], Miki Ohira[5], Masahiro Inoue[6], Hajime Kageyama[7], Sana Yokoi[7], Naokatsu Saeki[2] & Akira Nakagawara[1]

[1]Division of Biochemistry and Innovative Cancer Therapeutics, Chiba Cancer Center Research Institute, 666-2 Nitona, Chuo-ku, Chiba 260-8717, Japan, [2]Department of Neurological Surgery, School of Medicine, Chiba University, 1-8-1 Inohana, Chuo-ku, Chiba 260-8670, Japan, [3]Division of Neurosurgery, Chiba Cancer Center, 666-2 Nitona, Chuo-ku, Chiba 260-8717, Japan, [4]Division of Surgical Pathology, Chiba Cancer Center, 666-2 Nitona, Chuo-ku, Chiba 260-8717, Japan, [5]Laboratory of Cancer Genomics, Chiba Cancer Center Research Institute, 666-2 Nitona, Chuo-ku, Chiba 260-8717, Japan, [6]Department of Biochemistry, Osaka Medical Center for Cancer and Cardiovascular Diseases, 1-3-3 Nakamichi, Higashinari-ku, Osaka 537-8511, Japan, [7]Cancer Genome Center, Chiba Cancer Center Research Institute, 666-2 Nitona, Chuo-ku, Chiba 260-8717, Japan.

Glioblastoma multiforme (GBM) is a highly invasive and chemoradioresistant brain malignancy. Temozolomide (TMZ), a DNA-alkylating agent, is effective against GBM and has become the standard first-line drug. However, the mechanism by which TMZ regulates the progression of GBM remains elusive. Here, we demonstrate that TMZ targets TAp63, a p53 family member, inducing its expression to suppress the progression of human GBM. High levels of *TAp63* expression in GBM tissues after TMZ treatment was an indicator of favourable prognosis. In human GBM cells, TMZ-induced TAp63 directly repressed *MYC* transcription. Activation of this TAp63-*MYC* pathway by TMZ inhibited human GBM progression both *in vitro* and *in vivo*. Furthermore, downregulation of *MYC* mRNA levels in recurrent GBMs after TMZ treatment correlated with better patient survival. Therefore, our results suggest that the TAp63-mediated transcriptional repression of *MYC* is a novel pathway regulating TMZ efficacy in GBM.

Glioblastoma multiforme (GBM) has been resistant to a variety of chemotherapeutic regimens for the last half-century and the average survival duration of patients was previously about 12 months[1,2]. In 2005, however, temozolomide (TMZ) was reported to be effective against GBM and to increase the survival period by an average of three months[3]. The survival advantage conferred by TMZ is largely restricted to GBMs with a methylated promoter status of the DNA-repair gene O^6-methylguanine-DNA methyltransferase (*MGMT*)[4]. MGMT repairs cytotoxic O^6-methylguanine adducts induced by TMZ, and thus the expression of *MGMT* contributes to TMZ-resistance in GBM[4,5]. Nevertheless, the molecular mechanism by which TMZ achieves its effect on GBM has remained elusive[2,6].

The p53 tumour suppressor family includes p63 and p73 members[7–9]. The TAp63 and TAp73 isoforms, which bear transactivation domain, function similarly to the p53 tumour suppressor by inducing apoptosis following DNA damage[10], while ΔNp63 and ΔNp73, which lack this domain, act as oncogenes[11]. The p53 signalling pathway is often altered in human GBM[12]; however, there have been no reports on the function of p63 and p73 in GBM. Therefore, we focused on the roles of p63 and p73 in GBM to investigate the mechanisms of DNA damage-induced activation of the other p53 family members following TMZ treatment. In this study, we show that TMZ activates TAp63 to repress *MYC* transcription, and that the downregulation of *MYC* by TAp63 augments the efficacy of TMZ in human GBM by suppressing proliferation and invasion.

Results

High TAp63 expression correlates with favorable prognosis in human GBM. To investigate the expression levels of p63 and p73 in human GBM, 69 newly diagnosed malignant gliomas (59 GBMs; 7 anaplastic astrocytomas; 3 anaplastic oligoastrocytomas) were selected for RNA and DNA analyses (Supplementary Table S1). Forty-nine cases had received procarbazine, ACNU and vincristine (PAV) therapy and twenty had

received TMZ therapy. First, our clinical data showed that TMZ treatment significantly prolonged the survival period of patients with malignant glioma ($P = 0.0394$; Supplementary Fig. S1a), and that high levels of *MGMT* expression were significantly associated with unfavourable prognoses ($P = 0.0015$; Supplementary Fig. S1b). Following quantitative RT-PCR for the analysis of *TAp63* and *TAp73* expression, the samples were divided into groups with high or low levels of *TAp63* (Fig. 1a) and *TAp73* (Supplementary Fig. S2) based on their respective expression levels in a normal adult brain. Kaplan–Meier cumulative survival curves showed that high *TAp63* expression was significantly associated with prolonged survival ($P = 0.0373$; Fig. 1b). In contrast, the levels of *TAp73* expression showed no prognostic potential (Supplementary Fig. S2). Therefore, from here on we focused on *TAp63* and selected the 20 TMZ-treated GBM samples to perform immunohistochemical staining for p63. We found that p63 immunopositivity (Fig. 1c) was significantly associated with better recurrence-free survival ($P = 0.0066$, Fig. 1d), and as *ΔNp63* mRNA was not detectable in these samples (data not shown), the positive p63 immunohistochemical staining may largely reflect the expression levels of TAp63 protein. Therefore, a high expression level of TAp63 is a favourable prognostic indicator of human GBM for cases that undergo TMZ treatment.

TAp63 directly represses *MYC* transcription in response to TMZ. Since other DNA damaging agents activate TAp63 by inducing its mRNA expression[13], we next investigated the role of TMZ in TAp63 expression. The steady-state mRNA levels of *TAp63* in four human GBM cell lines were analysed (Supplementary Fig. S3a), and *TAp63* isoforms was the major TAp63 isoform expressed (Supplementary Fig. S3b). TMZ stimulated TAp63 expression in both *TP53* mutant (YH-13) and wild-type (U87MG) cells, and induced the expression of TAp63 target genes, including *BAX*, *CDKN1A* (*p21*) and *MDM2* (Fig. 2a; Supplementary Fig. S4). In recent reports on functional network modelling analyses of GBM, a significant association between the p53 and MYC pathways has been suggested[14,15]. In addition, deletions of *TP53* and *PTEN* in murine brains caused the spontaneous development of GBM with a simultaneous induction of *MYC*[16]. Therefore, we examined the expression of *MYC* in TMZ-treated GBM. Interestingly, TMZ induced *TAp63* expression and suppresses *MYC* expression in a dose-dependent manner in both U87MG and YH-13 cells (Fig. 2a). Immunoblotting also showed an increase in TAp63 with suppression of MYC (Fig. 2b). Since p53 is reported to directly repress *MYC* transcription[17,18], we investigated whether TAp63 could regulate the transcription of *MYC*. Regardless of the status of *TP53*, siRNA knockdown of *TAp63* induced MYC expression at both the mRNA (Fig. 2c; Supplementary Fig. S5a) and protein (Fig. 2d) levels, whereas *TAp63* overexpression suppressed *MYC* (Fig. 2e; Supplementary Fig. S5b) and induced *BAX*, *CDKN1A* and *MDM2* (Supplementary Fig. S6a,b). *MYCN* levels remained unaffected in GBM cell lines (Supplementary Fig. S7a,b). To further confirm if TAp63-mediated suppression of *MYC* occurred in primary GBM cells, we introduced

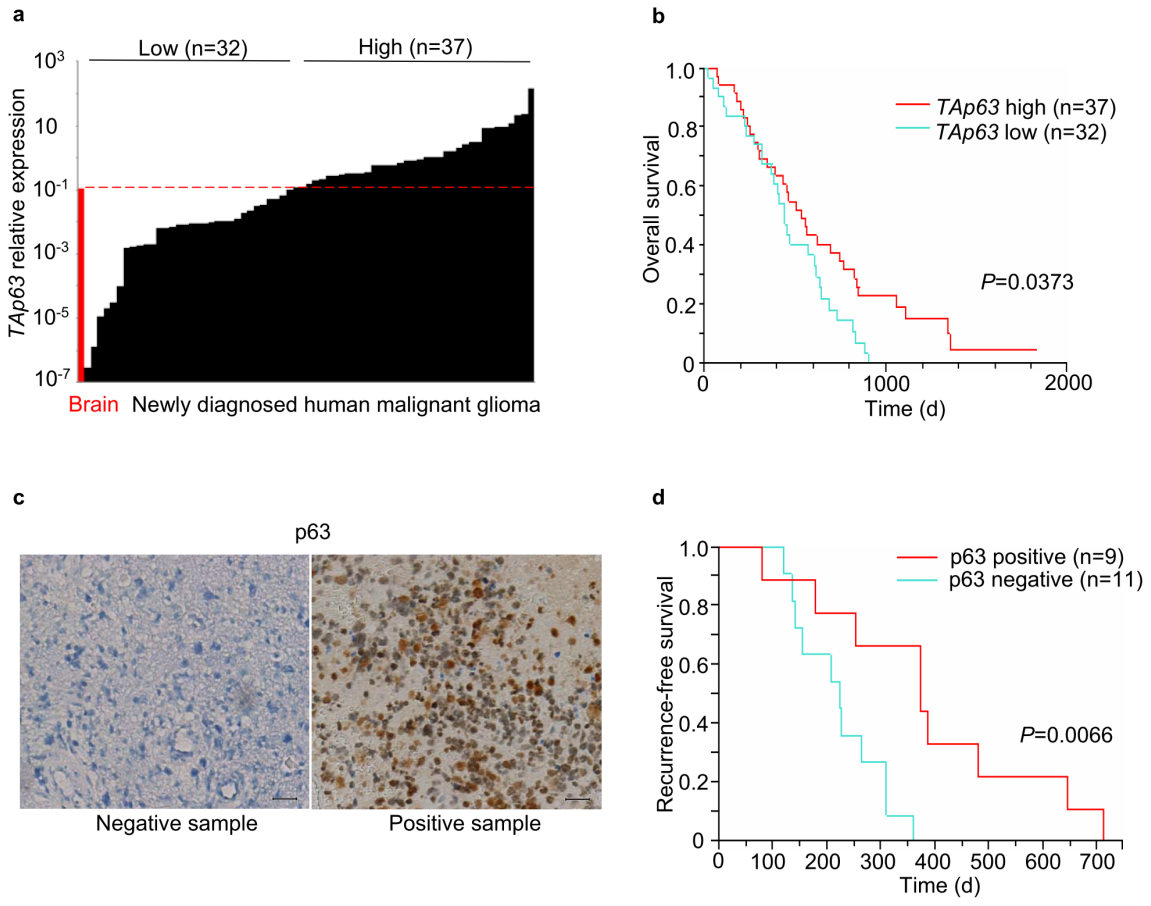

Figure 1 | High TAp63 expression correlates with favourable prognoses in human GBM. (a) *TAp63* mRNA expression detected by quantitative RT-PCR (qRT-PCR) in 69 newly diagnosed malignant glioma samples (59 GBM; 7 anaplastic astrocytoma; 3 anaplastic oligoastrocytoma). *TAp63* expression was normalised to *ACTB* mRNA, and designated high (n = 37) or low (n = 32) based on the normal human brain expression (dashed red line). (b) Overall survival of subjects with newly diagnosed malignant gliomas according to relative *TAp63* expression levels before chemotherapy (n = 69; high, n = 37; low, n = 32). *P* value by log-rank test. (c) p63 immunohistochemical staining in human GBM. Scale bar, 50 μm. (d) Recurrence-free survival of 20 TMZ-treated GBM subjects according to p63 immunohistochemical staining in newly diagnosed samples. *P* values by log-rank test.

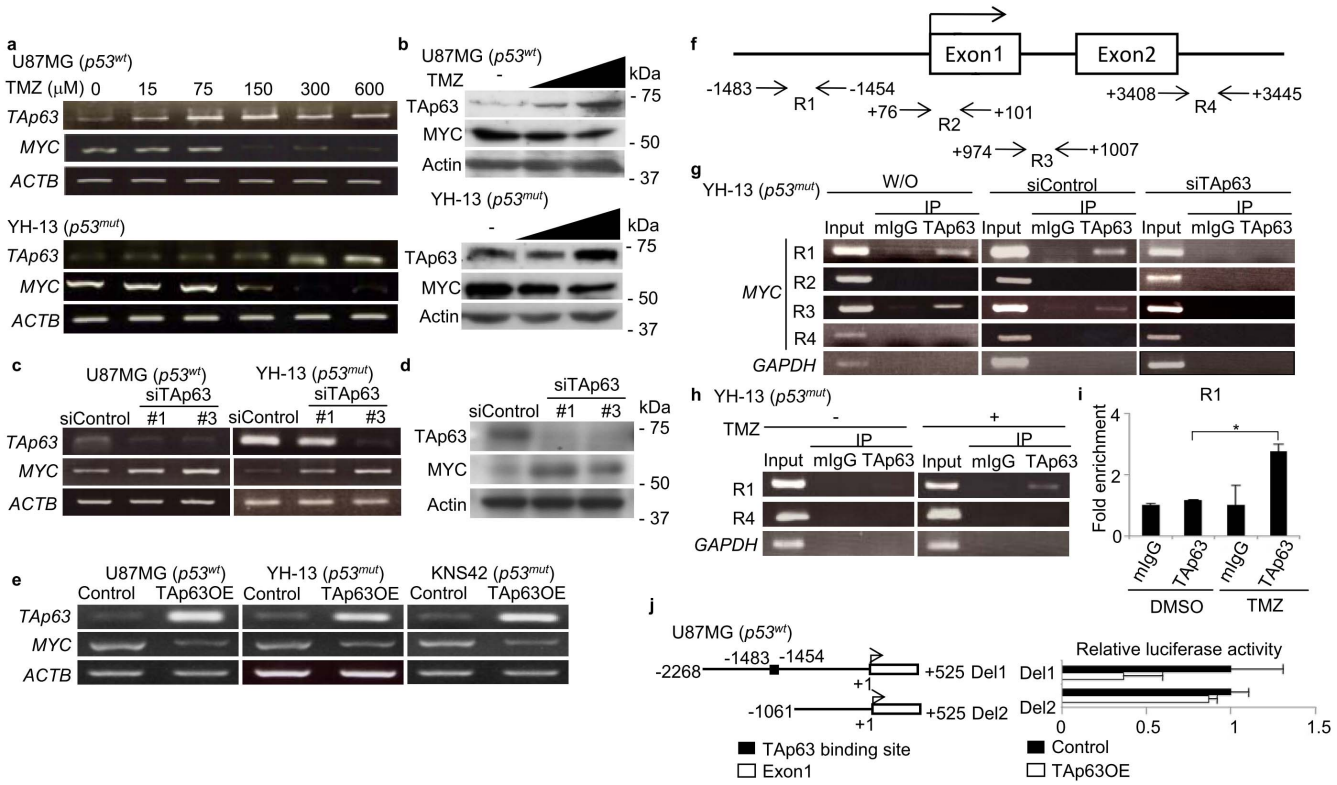

Figure 2 | TMZ-induced TAp63 suppresses *MYC* expression in human GBM cells. (a) *TAp63* and *MYC* mRNA levels in GBM cells with increasing TMZ concentrations, 24 h. (b) Immunoblot of TAp63 and MYC from GBM cells treated with increasing concentrations of TMZ, 24 h. (c) RT-PCR analyses of relative *MYC* expression in U87MG and YH-13 cells following siTAp63 transfection, normalised to *ACTB* mRNA. (d) Analysis of MYC expression in YH-13 cells transfected with siControl or siTAp63 by western blotting. (e) RT-PCR analyses showing *MYC* suppression after *TAp63α* overexpression in GBM cell lines. (f) Positions of PCR primer sets R1, R2, R3 and R4 for the chromatin immunoprecipitation (ChIP) assays. (g) Identification of the TAp63-binding region in the *MYC* promoter by ChIP assays. YH-13 cells were transfected with or without indicated siRNAs. Genomic DNA was amplified by PCR using the indicated primers. (h) Semi-quantitative PCR and (i) quantitative PCR of ChIP assays showing endogenous TAp63 recruitment onto the *MYC* promoter after 24 h TMZ treatment, 150 μM. $^*P < 0.005$ (two-tailed *t*-test). (j) Luciferase activity of *MYC* reporters after lentiviral *TAp63α* or GFP infection of U87MS cells. Data shown as the fold change in the luciferase activity compared with control cells.

the use of cancer tissue-originated spheroids (CTOS) composed of pure tumor cells derived directly from the GBM tissue[19]. As shown in Supplementary Fig. S8, the TAp63-*MYC* regulatory pathway was intact in the CTOS. To examine whether TAp63 directly represses *MYC* transcription, we performed a chromatin immunoprecipitation (ChIP) assay. We designed four primer sets (R1, R2, R3 and R4) to amplify the indicated genomic regions of the putative TP53 binding sequence (Fig. 2f). Our results showed that endogenous TAp63 was recruited to the upstream promoter and the intron 1 region of the *MYC* gene in YH-13 cells, but not intron 2, which has been previously shown as a p53-binding site[18] (Fig. 2g). In response to TMZ treatment, the amount of TAp63 recruited onto the *MYC* promoter was significantly increased (Fig. 2h,i), however, there was no increase in TAp63 recruitment onto intron 1 (Supplementary Fig. S9). *TAp63* overexpression in YH-13 and U87MG cells inhibited *MYC* promoter activity (Fig. 2j; Supplementary Fig. S10), suggesting that TMZ stimulates the TAp63-mediated repression of *MYC* transcription in GBM cells.

The TAp63-*MYC* pathway regulates sphere formation and invasion in GBM. *MYC* is a regulator of stemness in glioma, and its expression is required for glioma cell neurosphere formation[20]. Consistent with these notions, *TAp63* knockdown increased both the number and size of YH-13 neurospheres, while knockdown of *MYC* suppressed the sphere-forming ability (Fig. 3a,b). Moreover, the number of spheres formed by YH-13 cells co-transfected with both siTAp63 and siMYC was less than that of cells transfected with siTAp63 alone, suggesting that *MYC* induction by TAp63 knockdown contributes to the sphere-forming ability of tumour cells.

TAp63 also plays a critical role in the regulation of cancer invasion[21,22]. To assess whether the TAp63-*MYC* pathway also regulates invasion, *TAp63* and *MYC* were knocked down in YH-13 cells with siRNA for 24 and 48 h. Although knockdown of endogenous *TAp63* and *MYC* had no effect on cell proliferation by day 2 of culture (Fig. 3c), knockdown of *TAp63* alone significantly promoted the cellular invasion of YH-13 cells. Additionally, co-transfection of siTAp63 and siMYC decreased the percentage of invading cells compared to siControl-transfected cells (Fig. 3d), suggesting that TAp63 downregulates GBM invasion via *MYC* suppression.

Temozolomide suppresses tumour cell growth and invasion via TAp63 induction. We assessed whether TMZ affects the invasive property of GBM cells via the TAp63-*MYC* pathway. The treatment of U87MG cells with 75 μM TMZ inhibited cell proliferation and significantly inhibited cellular invasion on day 5 of exposure (Fig. 4a,b). Since apoptotic cell death was not observed under these experimental conditions (Supplementary Fig. S11), TMZ may have anti-invasive properties. Moreover, U87MG cells were transfected with the indicated siRNAs for *TAp63* and *MYC* and subjected to Boyden chamber invasion assays. *TAp63* knockdown in U87MG cells induced *MYC* mRNA expression and rescued the TMZ-inhibited cellular invasion, compared to the control (Fig. 4c). Next, to assess the antitumour effects of TAp63 *in vivo*, we knocked down

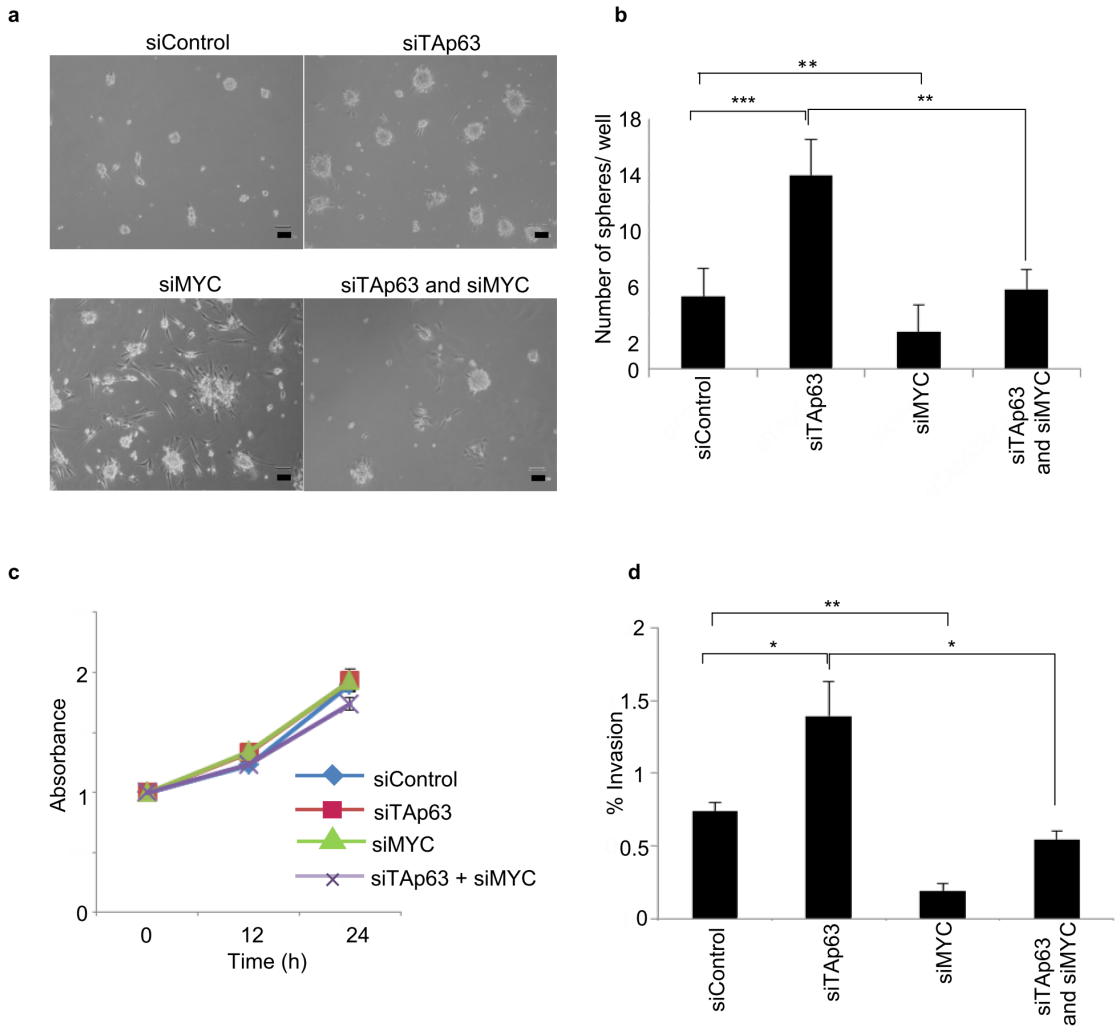

Figure 3 | TAp63-*MYC* pathway is critical for glioblastoma sphere-forming ability and invasion *in vitro*. (a) Sphere formation assay of YH-13 cells, showing induction of sphere-forming activity after knockdown of *TAp63* and *MYC*. (b) The graph indicates the differences in the sphere numbers per microscopic field at 400× magnification. The values represent the mean ± SD of triplicate samples from a single representative experiment (n = 9). $^{**}P < 0.0005$, $^{***}P < 0.00005$ (two-tailed *t*-test). (c) Cell viability assay of *TAp63* and *MYC* knockdown in YH-13 cells. (e) The graph indicates the percentage of YH-13 cells invading the Matrigel relative to control migration, following *TAp63* and *MYC* knockdown. $^{*}P < 0.05$, $^{**}P < 0.0005$ (two-tailed *t*-test).

TAp63 in the tumors of U87MG xenograft mouse models. Our results showed that TAp63 knockdown promotes tumour cell proliferation (Supplementary Fig. S12a,b). To investigate the role of TAp63 in TMZ efficacy, we implanted U87MG cells into the hind legs of mice (n = 4) and, 7 days later, injected siControl and siTAp63 into the palpable tumours, which were then treated with TMZ (15 mg/kg) intraperitoneally on the same day. At day 14, tumours subjected to siTAp63 knockdown with TMZ treatment were considerably larger compared to the control tumours, indicating a drug-resistant phenotype (Fig. 4d). Finally, we assessed whether the TMZ-induced activation of the TAp63-*MYC* pathway is associated with the clinical outcome of patients. To this end, we analysed the RNA from 20 paired (initially diagnosed tumour and recurrent tumour from the same patient) malignant glioma samples (17 GBMs, three anaplastic oligoastrocytomas) from TMZ-treated patients. The expression levels of *MYC* mRNA were significantly decreased after the treatment (Fig. 4e). Furthermore, the subgroup with decreased *MYC* expression after TMZ treatment showed significantly better overall survival (Fig. 4f). We performed a similar analysis using only the GBM mRNA data and both *TAp63* expression and *MYC* suppression indicated good prognoses (Fig S13a–f). Taken together, these findings suggest that the TMZ-mediated suppression of *MYC* via TAp63 activation is a key pathway for the drug's efficacy against GBM.

Discussion

In this study, we report that TAp63 regulates *MYC* transcription and tumor progression in TMZ-treated GBM. The study highlighted four points. First, TAp63 expression is a favourable prognostic factor in TMZ-treated GBM. Second, TMZ induces TAp63 to suppress growth and invasion. Third, TAp63 directly represses *MYC* expression in response to TMZ treatment, and fourth, *MYC* downregulation correlates with TMZ efficacy.

A possible mechanism of TMZ action could be that TMZ induces *TAp63* expression in GBM cells, and in turn, activated TAp63 inhibits cellular invasion via suppression of *MYC* expression. These findings are consistent with the previous reports in which TAp63 suppresses invasion through coordinated transcriptional regulation of its downstream target genes such as *SERPINB5, CCNG2, BHLHE41* and *DICER1*[21–24].

A prior study on the regulatory mechanisms of p53 upon its downstream targets showed that in response to hypoxic stress, p53 is recruited onto intron 2 of the *MYC* gene to directly inhibit *MYC* transcription[18]. Our work has identified a critical role for TAp63 as

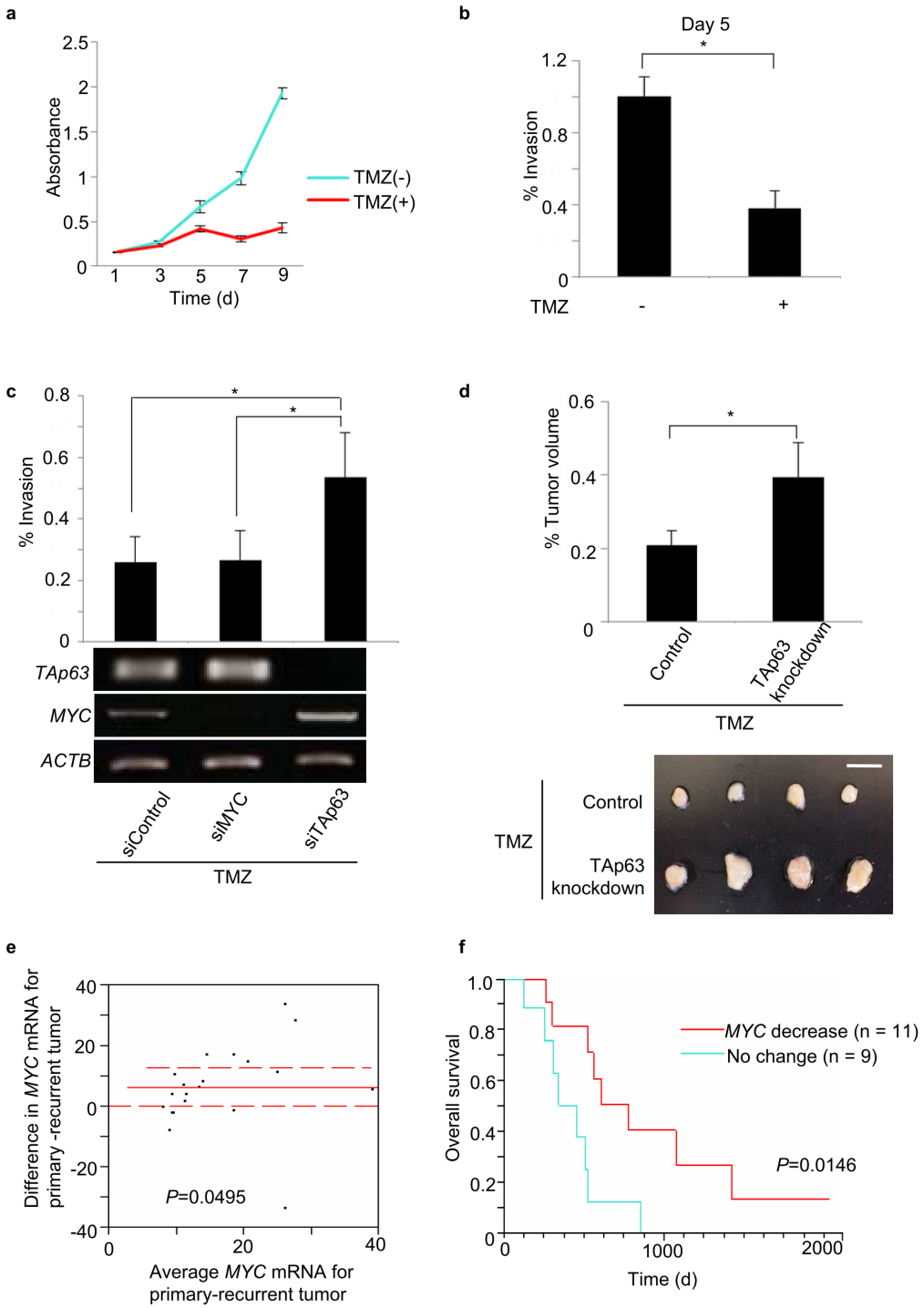

Figure 4 | TMZ inhibits GBM progression via the TAp63-*MYC* pathway. (a) Cell viability assay showing suppression of proliferation in cells treated with TMZ, 75 μM. (b) Cellular invasion was suppressed by day 5, at which point the treated and control cultures were adjusted to 5×10^4 cells/500 μl and subjected to Boyden chamber invasion assays. *$P < 0.05$ (two-tailed *t*-test). (c) Percentage of U87MG cells invading the Matrigel relative to control migration, following *TAp63* knockdown and TMZ treatment. Corresponding mRNA analysis. *$P < 0.05$ (two-tailed *t*-test). (d) Effect of *TAp63* knockdown on the U87MG cells treated with TMZ treatment at 14 days after subcutaneous transplantation in nude mice. The end volumes were compared to the volumes at implantation. Tumour growth was measured with callipers and calculated by the formula: volume = length (A) × width (B) × width (B) × 0.5, where A and B are the long and short axes respectively. TMZ in PBS was administered intraperitoneally at 15 mg/kg once a week. Data are representative of five independent experiments (n = 4). *$P < 0.05$ by two-tailed *t*-test. Photographs in (d) are representative of n = 4 mice. Bar, 10 mm. (e) *MYC* downregulation in recurrent tumours after TMZ plus radiotherapy (n = 20; solid line: mean difference; dashed lines: 95% confidence interval. *P* value by paired *t*-test. (f) Overall survival according to *MYC* downregulation (≥1.5-fold decrease in primary/recurrent (p/r) *MYC* mRNA), post-TMZ treatment. *MYC* decrease: n = 11, mean p/r = 2.65 ± 0.31 s.d.; no change: n = 9, mean p/r = 0.9 ± 0.13 s.d. *P* value by log-rank test.

an alternative regulator of *MYC* in human GBM. Distinct from the p53-MYC regulatory mechanism, TAp63 is activated in response to TMZ-induced stress, and does not bind to intron 2 but is recruited onto the upstream promoter region of *MYC* to directly repress transcription. In addition, the interaction between the p53 and MYC signaling networks are important for cellular proliferation and differentiation in the prevention of GBM pathogenesis[14,15,17]. However p53 is functionally inactivated in many aggressive GBMs[12]. Therefore, the newly identified TAp63-*MYC* regulatory pathway may serve as an alternative activator of the p53-regulated tumour suppressive pathways[10,21,25,26].

Recently, there have been several reports on the role of p53 in TMZ resistance in GBM. TMZ activates p53 to induce apoptosis in GBM cells[27,28], and functional inactivation of the p53 pathway by overexpression of the α5β1 integrin contributes to TMZ resistance in high-grade glioma[27]. On the other hand, reports also suggest that p53 inactivation rather increases TMZ sensitivity in GBM cell lines[29] and *in vivo* xenograft models[30], and that the status of p53 is not a molecular predictor of the response to chemotherapy with TMZ[31]. These discrepancies indicate the existence of an alternative mechanism underlying TMZ resistance in GBM which is independent of the p53 status. Our present data show that the TAp63-*MYC* pathway contributes to TMZ sensitivity in both *p53*-wild type and -mutant GBM cells, and that the expression levels of *TAp63* and *MYC* are prognostic factors in TMZ-treated GBM.

In conclusion, our results clearly indicate that *MYC* is a novel TAp63 target gene and that the TAp63-*MYC* pathway has a crucial role in mediating suppression of GBM progression. Pharmacological targeting of the TAp63-*MYC* pathway may therefore provide new rational therapeutic strategies against TMZ-resistant GBMs.

Methods

Glioma tumour samples and tissue dissection. A total of 89 malignant glioma samples comprising of newly-diagnosed GBM (World Health Organization (WHO) grade 4, n = 59), newly-diagnosed anaplastic astrocytoma (WHO grade 3, n = 7), newly-diagnosed anaplastic oligoastrocytoma (WHO grade 3, n = 3) and 20 recurrent malignant gliomas (17 GBMs, 3 anaplastic oligoastrocytomas) were collected between 1994 and 2011 and obtained from the Chiba Cancer Center upon receiving informed consent under an institutional review board-approved protocol. The present project was approved by the Ethics Committee of the Faculty of Biology and Medicine at the Chiba Cancer Center (protocol 15–19). After surgery, the patients were treated according to previously described protocols[32]. Although procarbazine, ACNU and vincristine (PAV) were used for chemotherapy until 2006, TMZ was used from 2006 in our facility. The tumour samples were routinely processed using a BenchMark® XT automated slide-processing system (Ventana Medical Systems, USA) for optimization and performance evaluation of the immunohistochemical assay for p63 protein. Paraffin-embedded tissue sections on glass slides were baked prior to the deparaffinization step with EZ Prep™ (Ventana). The sections were then washed with a mixture of Immunoblock (Dainippon Sumitomo Pharma Co.) and reaction buffer, followed by incubation with a mouse anti-human p63 monoclonal antibody (clone 4A4, Dako). The tumour samples were divided into three specimens: immediately snap-frozen in liquid nitrogen; diagnostic frozen sections for the Department of Pathology; and formalin-fixed paraffin-embedded sections. The specimens were homogenised using a rotor/stator homogenizer. DNA and RNA were extracted from the patient samples as previously described[33]. Total RNA was extracted from three healthy human brain tissue samples purchased from separate sources, Clontech, Stratagene and Zyagen, and the highest p63-expressing sample was used as the threshold standard. A newly diagnosed GBM specimen (supplied by Chiba Cancer Center) was used to generate cancer tissue-originated spheroid cultures as described previously[19].

Cell lines and specimen collection. GBM cell lines were purchased from the American Type Culture Collection (U87MG) and Health Science Research Resources Bank (YH-13, KNS-42 and SF126). The cell lines were cultured in modified Eagle's medium containing 20% (YH-13), 5% (KNS42) or 10% (U87MG and SF126) heat-inactivated foetal bovine serum (Invitrogen).

Temozolomide (TMZ) treatment. TMZ was purchased from LKT Laboratories Inc., and freshly prepared for experimental use. TMZ was added at the final concentrations 24 h after cell seeding for each experiment.

RT-PCR and qRT-PCR. The primers are described in the *SI Methods*.

Gene knockdown assay. The following gene-specific siRNAs were purchased: siTAp63-1, sense 5′-CAGCUAUAUGUUCAGUUCTT-3′ and antisense 5′-GAA CUGAACAUAUAGCUGTT-3′; siTAp63-3, sense 5′-CAGAAGAUGGUGCG ACAAATT-3′ and antisense 5′-UUUGUCGCACCAUCUUCUGTT-3′ from Sigma; siMyc-26 for CGAUGUUGUUUCUGUGGAA and siMyc-29 for CUACCAGGC UGCGCGCAAA from Thermo Scientific. The control siRNA (Mission siRNA Universal Negative Control SIC-001) was purchased from Sigma. All transfections were performed using Lipofectamine™ RNAiMax (Invitrogen). The transfections were carried out twice, with reverse transfection immediately following cell count to 1×10^5 cells/ml and forward transfection 24 h after reverse transfection.

Overexpression of TAp63 in human GBM cells. *TAp63α* was fused to the FLAG epitope at the NH_2 terminus and cloned into the lentiviral pHR vector. The lentivirus was produced by cotransfecting pHR, pCMVR and pMDG plasmids into HEK293T cells using the FuGENE HD reagent (Roche). At 12 and 24 h after transfection, the viral supernatants were collected and mixed with GBM cells.

Western blot assay. We resolved cell proteins by SDS-PAGE prior to electroblotting onto a PVDF membrane. We incubated the membranes with the following primary antibodies overnight: anti-p63 (4A4) (1 : 1000; sc-8431, Santa Cruz Biotechnology), anti-Myc (N-262) (1 : 2000; sc-764, Santa Cruz Biotechnology, Santa Cruz, CA, USA), and anti-Actin (20-33) (1 : 4000; A5060, Sigma). The membranes were then incubated with a horseradish peroxidase-conjugated secondary antibody (anti-rabbit IgG #7074, 1 : 2000–1 : 4000 or anti-mouse IgG #7076, 1 : 2000; Cell Signaling Technology) and the bound proteins were visualized using a chemiluminescence-based detection kit (ECL and ECL pro kit; Amersham and PerkinElmer).

Chromatin immunoprecipitation (ChIP) assay. YH-13 cells transfected with siRNA or exposed to TMZ at increasing concentrations between 150–300 μM were harvested 24 h after the second transfection or after TMZ exposure. ChIP assays were performed with a ChIP assay kit (Millipore) according to the manufacturer's instructions using an anti-p63 antibody (clone (4A4) sc-8431, Santa Cruz Biotechnology) and normal mouse IgG (015-000-003, Jackson ImmunoResearch Laboratories Inc.). The primer sequences for the *MYC* promoter are described in the *SI Methods*.

Luciferase reporter assay. pBV-LUC Del1 (#16601) and Del2 (#16602) containing the *MYC* promoter regions at nucleotides −2268 to +525 and −1061 to +525 from the transcription start site, respectively, were obtained from Addgene. YH-13 and U87MG cells were seeded at 5×10^4 cells/well in a 24-well plate and allowed to adhere overnight. The cells were subjected to lentiviral infection on the following day with control pHR vector or pHR-*TAp63α* vector. At 54 h after infection, the cells were seeded in triplicate on 12-well plates at 1×10^5 cells/well and cultured for 24 h. They were then cotransfected with 400 ng of *MYC* luciferase reporter construct and 40 ng of *Renilla* TK with Lipofectamine 2000 (Invitrogen). At 18 h after the second transfection, the cells were harvested and the luciferase activity was determined using a dual-luciferase assay system (Promega) according to the manufacturer's instructions.

Migration and invasion assay. The invasive potential of GBM cells *in vitro* was measured by evaluating the number of invading cells using Matrigel-coated Transwell inserts (BD Biosciences) according to the manufacturer's instructions. YH-13 and U87MG cells transfected with siTAp63 and siMyc were seeded onto an insert with 8 μm pores (BD Biosciences) in a 24-well plate at 2×10^5 cells/ml. The cells were treated with 150 μM TMZ and counted 18 h after siRNA knockdown. Cells on the lower side of the membrane were fixed with 4% paraformaldehyde and stained using a Diff Quick Staining Kit (Sysmex).

Cell viability assay (MTT assay). Cell viability was quantified by the 3-(4, 5-dimethylthiazol-2-yl)-2, 5-diphenyltetrazolium bromide (MTT) method. Cells were collected and seeded in 96-well plates at 1×10^5 cells/well. After addition of 10 μl of MTT tetrazolium salt (Sigma) solution to each well, the plates were incubated in a CO_2 incubator. The absorbance of each well was measured using a Dynatech MR5000 plate reader with a test wavelength of 450 nm and a reference wavelength of 630 nm.

Sphere formation assay. We evaluated neurospheres derived from YH-13 cells transfected with the appropriate siRNA. After performing cell counts, we plated single cells in 60 mm non-coated dishes (2.5×10^5 cells/dish; Iwaki) to check the sphere morphology, and used a 96-well ultra-low cluster plate (2.5×10^4 cells/well; Costar) to count the spheres. The cells were allowed to proliferate in serum-free DMEM (Sigma) and F12 medium (Invitrogen) containing epidermal growth factor (Sigma) and 20 ng/ml basic fibroblast growth factor (Invitrogen) with 2% B27 supplement (Invitrogen). Half of the medium was replaced with fresh culture medium every 7 days.

Mouse xenograft models. Six- or seven-week-old male athymic BALB/c nu/nu mice were obtained from Japan SLC, Inc. The mice were anesthetized with intraperitoneal tribromoethanol (Wako) at 20 mg/kg body weight. U87MG cells mixed with an equal volume of Matrigel were implanted into the right and left hind legs. One week after tumour cell implantation, we injected 50 μl of Atelogene (Koken) with either control siRNA or siTAp63 (10 μM) into the U87MG xenografts. A total of 15 mg/kg TMZ in PBS was administered intraperitoneally once per week. Tumour growth was

measured with calipers and calculated by the formula: volume (V) = length (A) × width (B) × width (B) × 0.5. These studies were approved by the Committee for Animal Care at the Chiba Cancer Center Research Institute.

Statistical analysis. Data is presented as the mean ± the standard deviation. Statistical significances in the clinical data were calculated using Kaplan-Meier survival curves. Statistical analyses were performed with JMP® 10 (SAS institute Japan).

1. Chen, J., McKay, R. M. & Parada, L. F. Malignant glioma: lessons from genomics, mouse models, and stem cells. *Cell* **149**, 36–47 (2012).
2. Mrugala, M. M. & Chamberlain, M. C. Mechanisms of disease: temozolomide and glioblastoma - look to the future. *Nat. Clin. Pract. Oncol.* **5**, 476–486 (2008).
3. Stupp, R. *et al.* Radiotherapy plus concomitant and adjuvant temozolomide for glioblastoma. *N. Engl. J. Med.* **352**, 987–996 (2005).
4. Hegi, M. E. *et al.* MGMT gene silencing and benefit from temozolomide in glioblastoma. *N. Engl. J. Med.* **352**, 997–1003 (2005).
5. Shah, N. *et al.* Comprehensive analysis of *MGMT* promoter methylation: correlation with MGMT expression and clinical response in GBM. *PLoS One* **6**, e16146 (2011).
6. Beier, D., Schulz, J. B. & Beier, C. P. Chemoresistance of glioblastoma cancer stem cells - much more complex than expected. *Mol. Cancer* **10**, 128 (2011).
7. Osada, M. *et al.* Cloning and functional analysis of human p51, which structurally and functionally resembles p53. *Nat. Med.* **4**, 839–843 (1998).
8. Yang, A. *et al.* p63, a p53 homolog at 3q27-29, encodes multiple products with transactivating, death-inducing, and dominant-negative activities. *Mol. Cell* **2**, 305–316 (1998).
9. Kaghad, M. *et al.* Monoallelically expressed gene related to p53 at 1p36, a region frequently deleted in neuroblastoma and other human cancers. *Cell* **90**, 809–819 (1997).
10. Stiewe, T. The p53 family in differentiation and tumorigenesis. *Nat. Rev. Cancer* **7**, 165–168 (2007).
11. Deyoung, M. P. & Ellisen, L. W. p63 and p73 in human cancer: defining the network. *Oncogene* **26**, 5169–5183 (2007).
12. Cancer Genome Atlas Research Network. Comprehensive genomic characterization defines human glioblastoma genes and core pathways. *Nature* **455**, 1061–1068 (2008).
13. Suenaga, Y. *et al.* TATA-binding protein (TBP)-like protein is engaged in etoposide-induced apoptosis through transcriptional activation of human TAp63 gene. *J. Biol. Chem.* **284**, 35433–35440 (2009).
14. Aguda, B. D., Kim, Y., Kim, H. S., Friedman, A. & Fine, H. A. Qualitative network modeling of the Myc-p53 control system of cell proliferation and differentiation. *Biophys. J.* **101**, 2082–2091 (2011).
15. Bredel, M. *et al.* Functional network analysis reveals extended gliomagenesis pathway maps and three novel MYC-interacting genes in human gliomas. *Cancer Res.* **65**, 8679–8689 (2005).
16. Zheng, H. *et al.* p53 and Pten control neural and glioma stem/progenitor cell renewal and differentiation. *Nature* **455**, 1129–1133 (2008).
17. Ho, J. S., Ma, W., Mao, D. Y. & Benchimol, S. p53-dependent transcriptional repression of c-myc is required for G1 cell cycle arrest. *Mol. Cell Biol.* **25**, 7423–7431 (2005).
18. Krieg, A. J., Hammond, E. M. & Giaccia, A. J. Functional analysis of p53 binding under differential stresses. *Mol. Cell Biol.* **26**, 7030–7045 (2006).
19. Kondo, J. *et al.* Retaining cell-cell contact enables preparation and culture of spheroids composed of pure primary cancer cells from colorectal cancer. *Proc. Natl. Acad. Sci. USA* **108**, 6235–6240 (2011).
20. Wang, J. *et al.* c-Myc is required for maintenance of glioma cancer stem cells. *PLoS One* **3**, e3769 (2008).
21. Su, X. *et al.* TAp63 suppresses metastasis through coordinate regulation of Dicer and miRNAs. *Nature* **467**, 986–990 (2010).
22. Melino, G. p63 is a suppressor of tumorigenesis and metastasis interacting with mutant p53. *Cell Death Differ.* **18**, 1487–1499 (2011).
23. Kim, S., Han, J., Kim, J. & Park, C. Maspin expression is transactivated by p63 and is critical for the modulation of lung cancer progression. *Cancer Res.* **64**, 6900–6905 (2004).
24. Adorno, M. *et al.* A Mutant-p53/Smad complex opposes p63 to empower TGFβ-induced metastasis. *Cell* **137**, 87–98 (2009).
25. Sachdeva, M. *et al.* p53 represses c-Myc through induction of the tumor suppressor miR-145. *Proc. Natl. Acad. Sci. USA* **106**, 3207–3212 (2009).
26. Guo, X. *et al.* TAp63 induces senescence and suppresses tumorigenesis *in vivo*. *Nat. Cell Biol.* **11**, 1451–1457 (2009).
27. Janouskova, H. *et al.* Integrin α5β1 plays a critical role in resistance to temozolomide by interfering with the p53 pathway in high-grade glioma. *Cancer Res.* **72**, 3463–3470 (2012).
28. Zhang, W. B. *et al.* Activation of AMP-activated protein kinase by temozolomide contributes to apoptosis in glioblastoma cells via p53 activation and mTORC1 inhibition. *J. Biol. Chem.* **285**, 40461–40471 (2010).
29. Blough, M. D. *et al.* Effect of aberrant p53 function on temozolomide sensitivity of glioma cell lines and brain tumor initiating cells from glioblastoma. *J. Neurooncol.* **102**, 1–7 (2011).
30. Dinca, E. B. *et al.* p53 small-molecule inhibitor enhances temozolomide cytotoxic activity against intracranial glioblastoma xenografts. *Cancer Res.* **68**, 10034–10039 (2008).
31. Weller, M. *et al.* Molecular predictors of progression-free and overall survival in patients with newly diagnosed glioblastoma: a prospective translational study of the German Glioma Network. *J. Clin. Oncol.* **27**, 5743-5750 (2009).
32. Iuchi, T. *et al.* Hypofractionated high-dose irradiation for the treatment of malignant astrocytomas using simultaneous integrated boost technique by IMRT. *Int. J. Radiat. Oncol. Biol. Phys.* **64**, 1317–1324 (2006).
33. Ohira, M. *et al.* Expression profiling using a tumor-specific cDNA microarray predicts the prognosis of intermediate risk neuroblastomas. *Cancer Cell* **7**, 337–350 (2005).

Acknowledgments

We would like to thank R. I. Selim, Y. Kaneko, D. Matsumoto and K. Ando for technical support, A. Sada and N. Kitabayashi for DNA and RNA extractions, Y. Nakamura for sequencing support, R. Takano for lentivirally expressed TAp63α, and E. Isogai for helpful discussions and experimental assistance with mice throughout the course of this study. This work was supported in part by a grant-in-aid from the Ministry of Health, Labour and Welfare for the Third Term Comprehensive Control Research for Cancer, Japan, and a grant-in-aid for Scientific Research on Priority Areas from the Ministry of Education, Culture, Sports, Science and Technology, Japan.

Author contributions

T.Y. and Y.S. designed, performed and analysed cellular and animal experiments and wrote the manuscript. T.I. collected clinical samples and analysed clinical data. J.A. and A.T. performed and analysed cellular and animal experiments and wrote the manuscript. M.I. and A.A. performed pathological analyses of surgical tissue samples. M.O. assisted with figures and experimental design. M.I. supported the generation of cancer tissue originated-spheroid cultures. H.K. and S.Y. performed genomic mutation search experiments. N.S. assisted in experiments and associated clinical annotations. A.N. designed and supervised the experiments, analysed data, and wrote and edited the manuscript.

Additional information

Supplementary information accompanies this paper at http://www.nature.com/scientificreports

Competing financial interests: The authors declare no competing financial interests.

How to cite this article: Yamaki, T. *et al.* Temozolomide suppresses *MYC* via activation of TAp63 to inhibit progression of human glioblastoma. *Sci. Rep.* **3**, 1160; DOI:10.1038/srep01160 (2013).